Figure S1

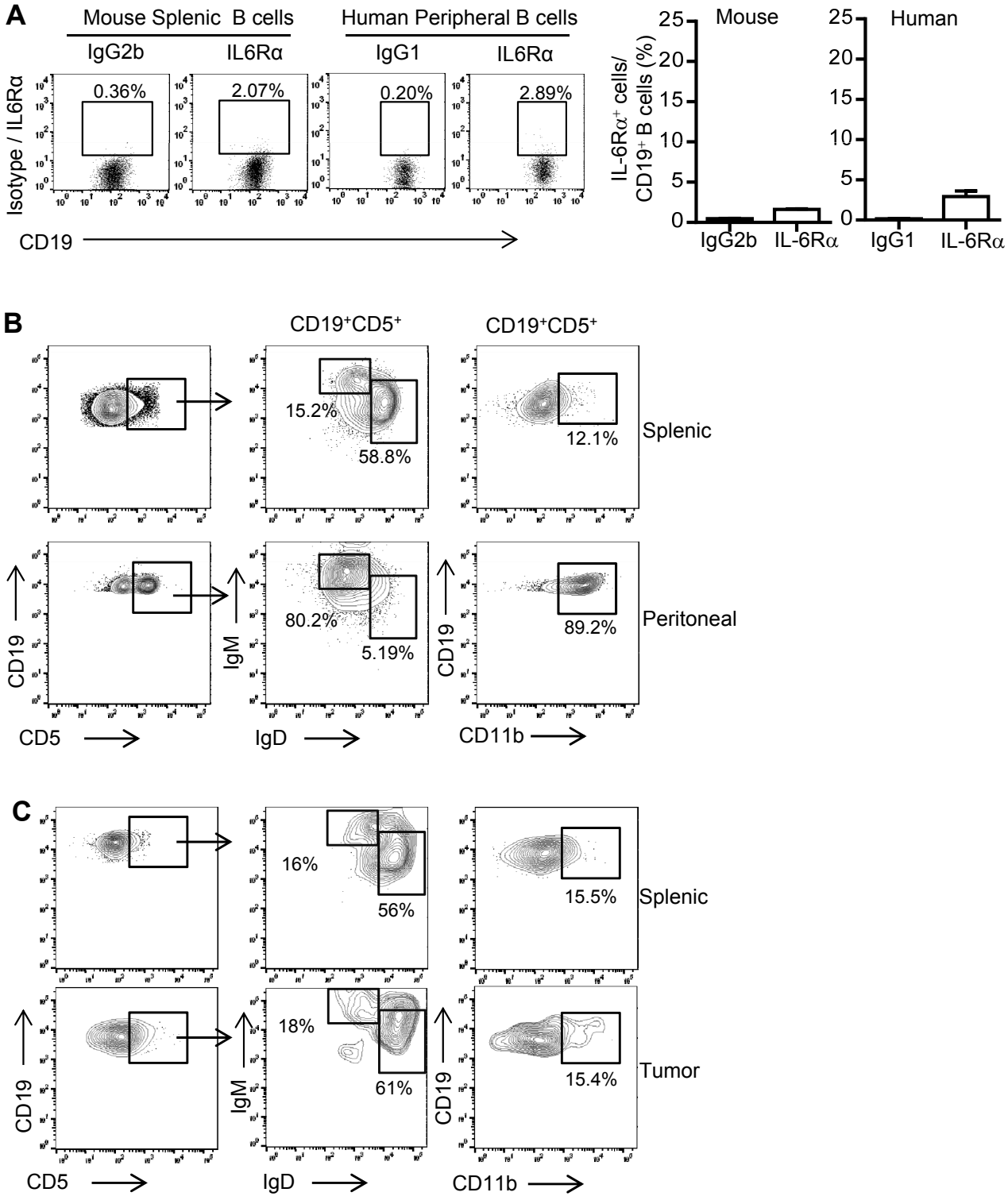
A
Mouse Splenic B cells
Human Peripheral B cells
IgG2b
IL6Rα
IgG1
IL6Rα
0.36%
2.07%
0.20%
2.89%
Isotype / IL6Rα
CD19
Mouse
Human
IL-6Rα+ cells/ CD19+ B cells (%)
25
20
15
10
5
0
IgG2b
IL-6Rα
IgG1
IL-6Rα
B
CD19+CD5+
CD19+CD5+
15.2%
58.8%
12.1%
Splenic
80.2%
5.19%
89.2%
Peritoneal
CD19
CD5
IgM
IgD
CD19
CD11b
C
16%
56%
15.5%
Splenic
18%
61%
15.4%
Tumor
CD19
CD5
IgM
IgD
CD19
CD11b

Figure S2

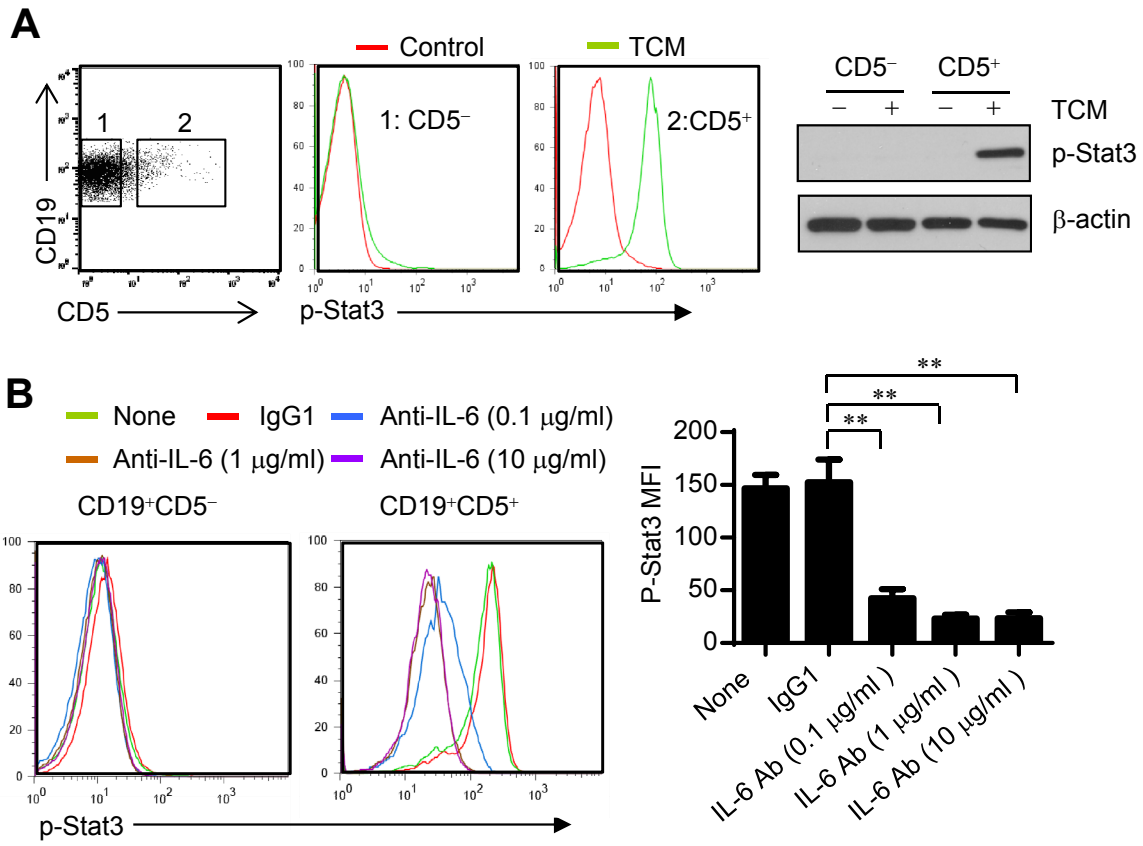
A
Control
TCM
1
2
CD19
CD5
1: CD5⁻
2:CD5⁺
p-Stat3
CD5⁻
CD5⁺
TCM
p-Stat3
β-actin
B
None
IgG1
Anti-IL-6 (0.1 μg/ml)
Anti-IL-6 (1 μg/ml)
Anti-IL-6 (10 μg/ml)
CD19⁺CD5⁻
CD19⁺CD5⁺
p-Stat3
P-Stat3 MFI
**
**
**
None
IgG1
IL-6 Ab (0.1 μg/ml)
IL-6 Ab (1 μg/ml)
IL-6 Ab (10 μg/ml)

Figure S3

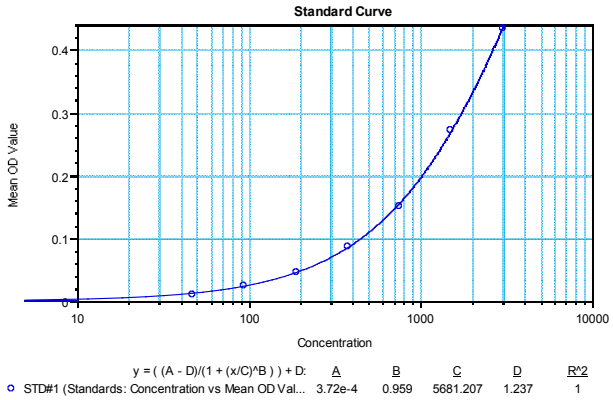

OD 450 value (Mouse sIL-6 ELISA)

Group	IL-6 stimulation				TCM treatment	
	$CD5^{+}IL\text{-}6R^{+}$	$CD5^{-}IL\text{-}6R^{+}$	$CD5^{+}IL\text{-}6R^{-}$	$CD5^{-}IL\text{-}6R^{-}$	$CD19^{+}CD5^{+}$	$CD19^{+}CD5^{-}$
OD(450 nm)	-0.002	-0.004	-0.008	-0.006	-0.005	-0.003

Figure S4

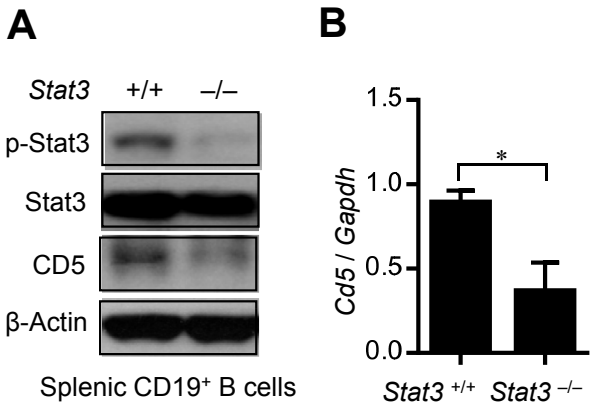
A
Stat3 +/+ –/–
p-Stat3
Stat3
CD5
β-Actin
Splenic CD19+ B cells
B
1.5
1.0
0.5
0.0
Cd5 / Gapdh
*
Stat3 +/+
Stat3 –/–

Figure S5

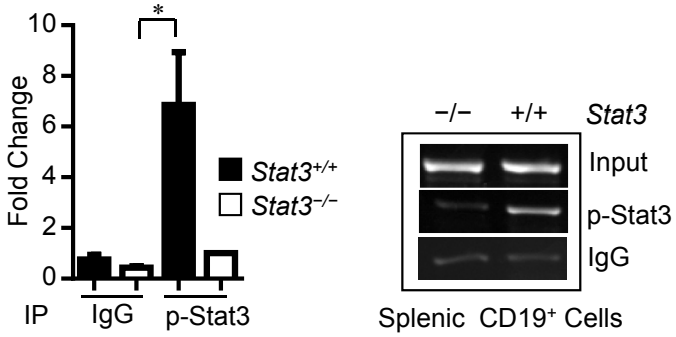
*
10
8
6
4
2
0
Fold Change
Stat3+/+
Stat3−/−
IP
IgG
p-Stat3
−/−
+/+
Stat3
Input
p-Stat3
IgG
Splenic CD19+ Cells

Figure S6

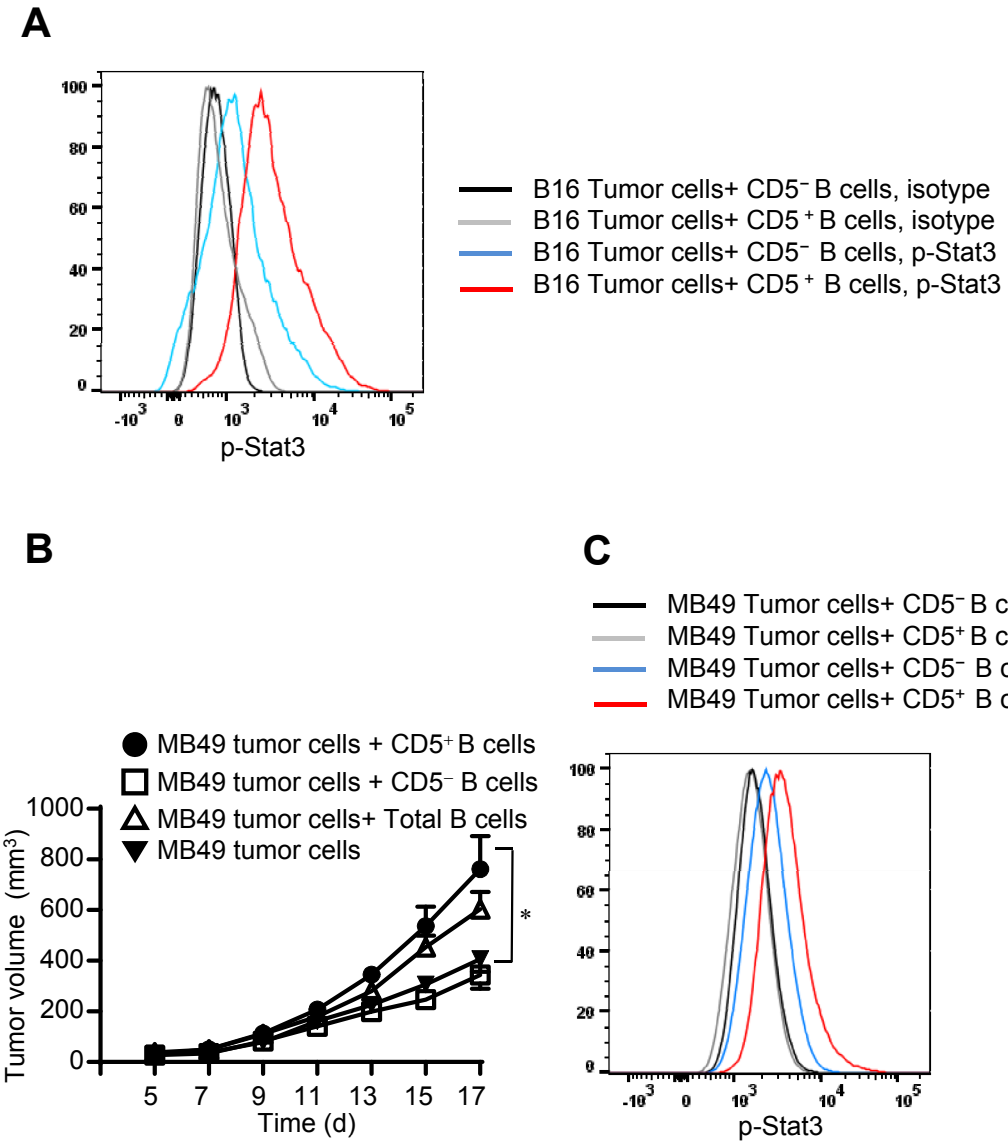
A
B16 Tumor cells+ CD5⁻ B cells, isotype
B16 Tumor cells+ CD5⁺ B cells, isotype
B16 Tumor cells+ CD5⁻ B cells, p-Stat3
B16 Tumor cells+ CD5⁺ B cells, p-Stat3
p-Stat3
B
MB49 tumor cells + CD5⁺ B cells
MB49 tumor cells + CD5⁻ B cells
MB49 tumor cells+ Total B cells
MB49 tumor cells
Tumor volume (mm³)
Time (d)
*
C
MB49 Tumor cells+ CD5⁻ B cells, isotype
MB49 Tumor cells+ CD5⁺ B cells, isotype
MB49 Tumor cells+ CD5⁻ B cells, p-Stat3
MB49 Tumor cells+ CD5⁺ B cells, p-Stat3
p-Stat3

Figure S7

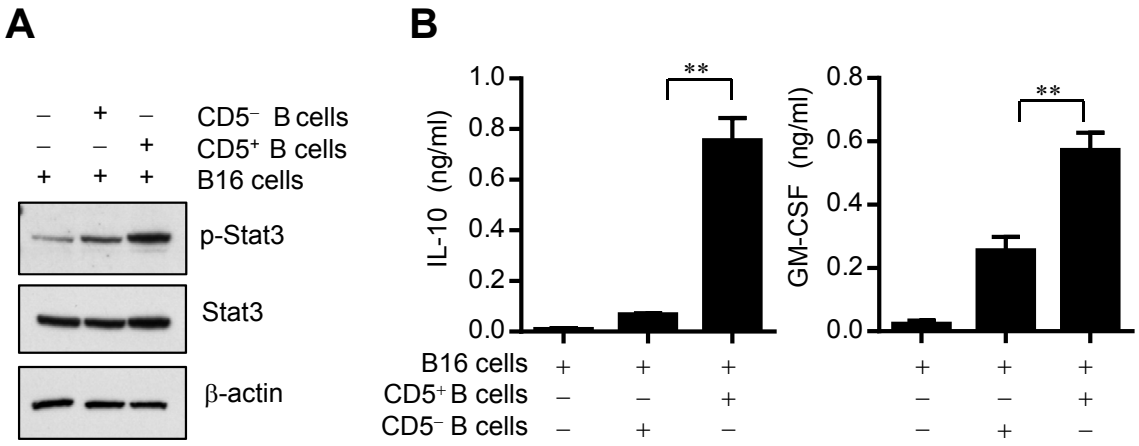
A
– + – CD5⁻ B cells
– – + CD5⁺ B cells
+ + + B16 cells
p-Stat3
Stat3
β-actin
B
IL-10 (ng/ml)
1.0
0.8
0.6
0.4
0.2
0.0
**
GM-CSF (ng/ml)
0.8
0.6
0.4
0.2
0.0
**
B16 cells + + + + + +
CD5⁺ B cells – – + – – +
CD5⁻ B cells – + – – + –

SUPPLEMENTAL FIGURE LEGENDS

Figure S1. Characterization of IL-6Rα$^+$ B cells and CD5$^+$ B cells. Related to Figure 1. (A) Representative dot plots (left) and statistical results (right) of flow cytometry analyses showing IL-6Rα$^+$ cell frequencies within CD19$^+$ B cells. Data are shown as means ± SEM (n = 15 and 9 for mouse and human samples, respectively). (B-C) Flow cytometry analyses of CD5$^+$ B cells from spleen and peritoneal cavity of naïve C57BL/6 mice (B), and from spleen and tumors harvested from B16 tumor bearing C57BL/6 mice (C). Single-cell suspensions derived from mouse spleen, peritoneal cavity (B) and tumor (C) were stained with anti-CD19, CD5, IgM, IgD and CD11b, to detect mouse CD5$^+$IgM^{hi}gD^{low} cells as well as CD5$^+$CD11b$^+$ B1 cells.

Figure S2. CD5 is crucial for IL-6-dependent Stat3 activation in B cells induced by TCM. Related to Figure 1. (A) Stat3 activation induced by 5% TCM in mouse splenic CD5$^+$ and CD5$^-$ B cells, as evaluated by flow cytometry (left) and western blotting of FACS-sorted cells (right). (B) Representative histograms of flow cytometry showing the inhibitory effect by IL-6 antibody neutralization on Stat3 activation induced in CD5$^+$ and CD5$^-$ B cells (left). Bar graphs indicate statistical results of mean fluorescence intensity (MFI), means ± SEM (right; n = 3).

Figure S3. sIL-6Rα does not contribute measurably to IL-6-induced CD5−associated Stat3 activation. Related to Figure 2. ELISA determining sIL-6Rα concentration in culture medium with either IL-6 or TCM.

Figure S4. Ablating Stat3 in mouse splenic and tumor-associated B cells abrogates CD5 expression. Related to Figure 5. (A-B) Western blotting (A) and real-time RT-PCR (B) measuring CD5 protein expression in splenic B cells from B16 tumor-bearing mice with or without *Stat3* ablation in CD19$^+$ cells, and CD5 mRNA level in CD19$^+$ B cells enriched from the tumors, respectively. Data represent means ± SEM of 3 independent experiments, each involving 6 pooled mice per group done in triplicates.

Figure S5. ChIP assay showing p-Stat3 binding to the *Cd*5 promoter. Related to Figure 5. Chromatins were prepared from splenic CD19$^+$ B cells of tumor-bearing mice. Quantitative real-time PCR (left) or regular PCR (right) showing the relative amounts of specific DNA fragments of *CD5* promoter after immunoprecipitating by p-Stat3/IgG and normalizing to the input. Results are means ± SEM (n = 3).

Figure S6. CD5$^+$ B cells significantly contribute to tumor cell Stat3 activation and tumor growth. Related to Figure 6. (A) Tumors grown from B16 tumor cells mixed with either CD5$^+$ B cells or CD5$^-$ B cells were harvested. Single-cell suspensions were subjected to flow cytometric analysis to detect p-Stat3 levels in tumor cells (gating was on tumor cells). (B) Growth curves of MB49 tumors implanted with CD5$^+$ or CD5$^-$ B cells in *Rag1*$^{-/-}$ mice. Representative results of 2 independent experiments (n = 6) are shown as means ± SEM ** $P < 0.01$. (C) Flow cytometry showing elevated p-Stat3 level in tumor cells derived from MB49 tumors grown in *Rag*$^{-/-}$ mice in the presence of either CD5$^+$ B cells or CD5$^-$ B cells.

Figure S7. CD5$^+$ B cells-mediated Stat3 activation in B16 tumor cells involves cytokines IL-10 and GM-CSF. Related to Figure 6. (A) Irradiated B16 tumor cells were co-cultured with CD5$^+$ or CD5$^-$ splenic B cells for 3 days, followed by cell lysate preparation of B16 tumor cells for Western blotting to detect p-Stat3. (B) Multiplex bead assay detecting IL-10 and GM-CSF production from irradiated B16 tumor cells co-cultured with CD5$^+$ or CD5$^-$ splenic B cells. Data represent means ± SEM (n = 3). $^{**}P <$ 0.01.